

Design of compressible and elastic N-doped porous carbon nanofiber aerogels as binder-free supercapacitor electrodes

Yi Yang, Yu-xin Liu, Yan Li, Bo-wen Deng, Bo Yin*, Ming-bo Yang

College of Polymer Science and Engineering, State Key Laboratory of Polymer Materials Engineering,

Sichuan University, Chengdu, Sichuan, People's Republic of China

*E-mail: yinbo@scu.edu.cn

1. Preparation of electrospun PAN/ZIF-8 fabrics

1.1. Synthesis of ZIF-8 nanoparticles

Typically, a solution of 2-methylimidazole (MeIM, 6.568 g) in 100 ml of methanol (MeOH) was rapidly poured into a solution of $\text{Zn}(\text{NO}_3)_2 \cdot 6\text{H}_2\text{O}$ (2.974 g) in 200 ml of MeOH under magnetic stirring at 25 °C for 2 h. Then the precipitate was collected by centrifugation and washed with methanol. ZIF-8 nanocrystals were finally dried under vacuum at 60 °C for 18 h.

1.2. Electrospinning of PAN/ZIF-8 fabrics

In a typical procedure, a dispersion consisting of 0.706 g ZIF-8 nanoparticles and 5 mL of N, N-dimethylformamide (DMF) was prepared by sonication, followed by the addition of 0.47 g of polyacrylonitrile (PAN, $M_w = 150000$) with vigorous stirring for 12 h. Then the precursor solution was loaded into a plastic syringe using a stainless-steel nozzle with a feed rate of 1 mL/h. The voltage between the needle tip and aluminum foil collector was 18 kV.

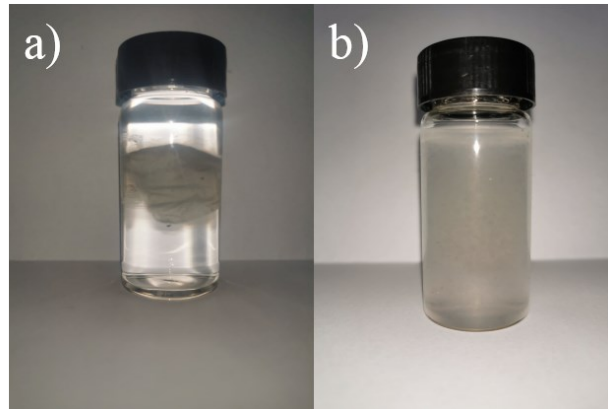


Fig. S1 Optical photographs of a) PAN/ZIF-8 membrane and b) homogenized PAN/ZIF-8 nanofibers dispersed in water/tert-butanol mixture

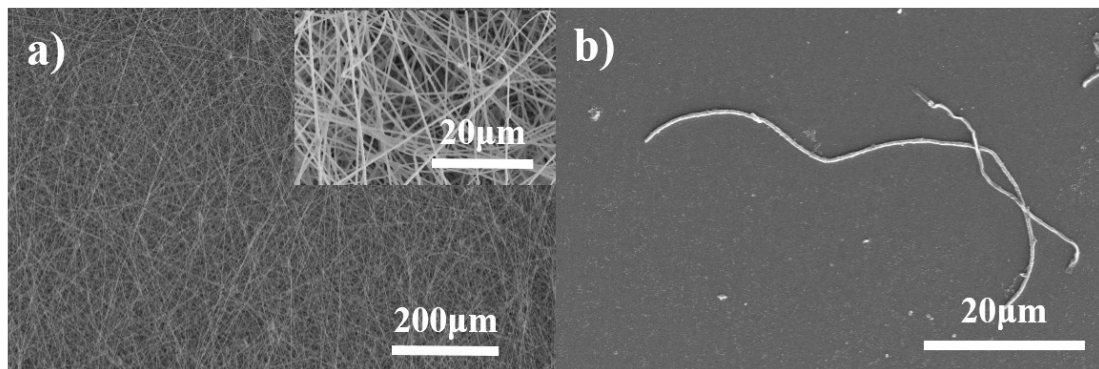


Fig. S2 SEM images of PAN/ZIF-8 membrane and homogenized PAN/ZIF-8 nanofibers

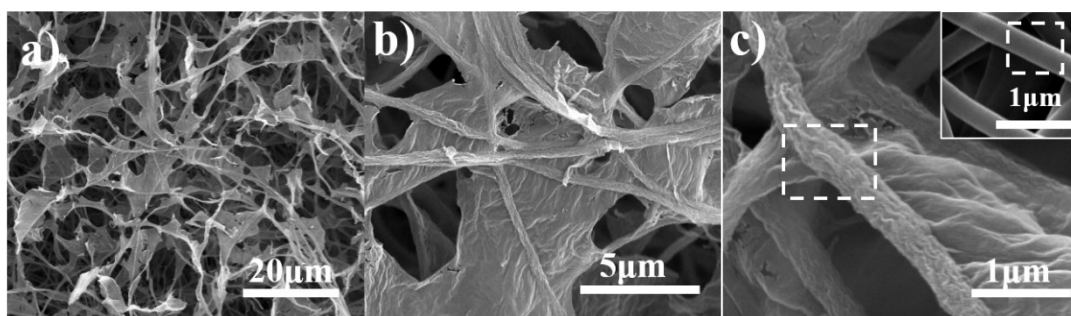


Fig. S3 a), b) and c) SEM images of rGO/CNFs. Inset in Fig. S3c is the SEM image of PAN-based CNFs

Fig. S3a, b and c were SEM pictures of rGO/PAN-based CNFs. It was prepared by mixing eletrospun PAN fibers and GO followed by carbonization at 800 °C in our

previous work. Through this part of work, we found that the GO platelet could wrap the nearby fibers after carbonation, which would fix these fibers to the platelet in Fig. S3b and give them a bearing surface. The picture inset in Fig. S3c was the appearance of PAN-based CNFs with a smooth surface, while the surface of rGO-wrapping fibers was corrugated due to rGO sheets which were wrapping on fibers. This behavior would endow the structure of rGO-wrapping fibers with certain mechanical strength. Thus, we introduced this structure to the CNF aerogel to connect and support the incompact and disconnected fibers, and thought it would bring some mechanical strength to the 3D architecture of aerogels and avoid the collapse of it.



Fig. S4 Optical photograph of the ultralight N-PCNF aerogel standing on a flower

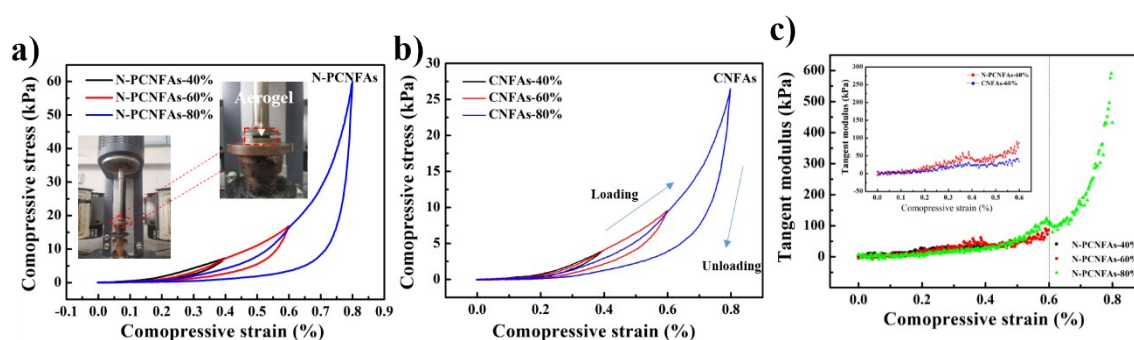


Fig. S5 Compressive mechanical property of N-PCNFAs and CNFAs. (a) Compressive stress (σ) versus compressive strain (ϵ) curves of N-PCNFAs. Inset: photograph of the aerogel in the holder of the rheometer. (b) σ - ϵ curves of CNFAs. (c) Tangent modulus

$(d\sigma/d\varepsilon)$ versus ε of N-PCNFAs at set ε maxima of 40%, 60% and 80%. Inset: comparison of the tangent modulus at set ε maxima of 60% of N-PCNFAs and CNFAs.

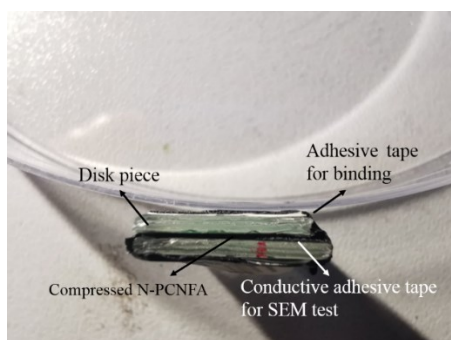


Fig. S6 Optical photograph of N-PCNFAs sandwiched between two disk pieces. This device was used to observe the compressed state of the cross section of N-PCNFAs by SEM. N-PCNFAs which was the same sample as that used for Fig. 2a was sandwiched between two disk pieces tightly to simulate the compressed state of N-PCNFAs as shown in Fig. 2h.

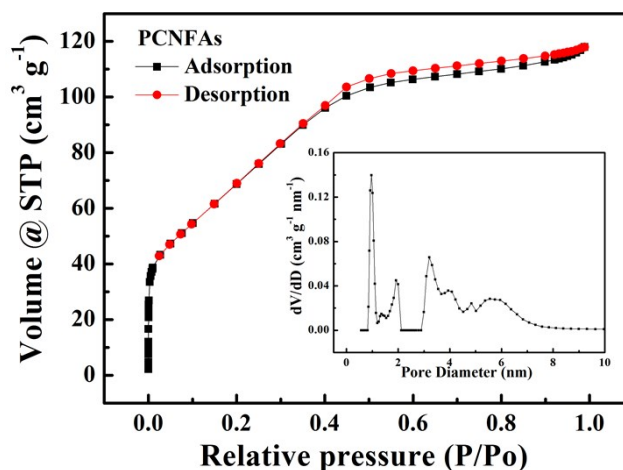


Fig. S7 Nitrogen adsorption-desorption isotherm of PCNFAs. The inset shows the corresponding pore size distribution (DFT).

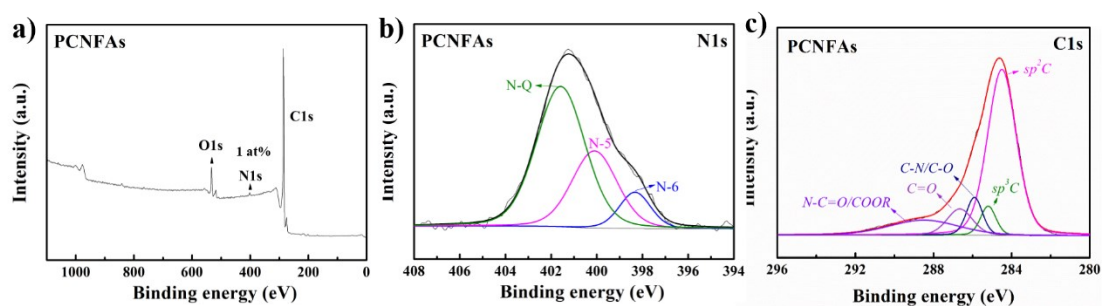


Fig. S8 (a) Full, (b) N1s and (c) C1s XPS spectra of PCNFAs

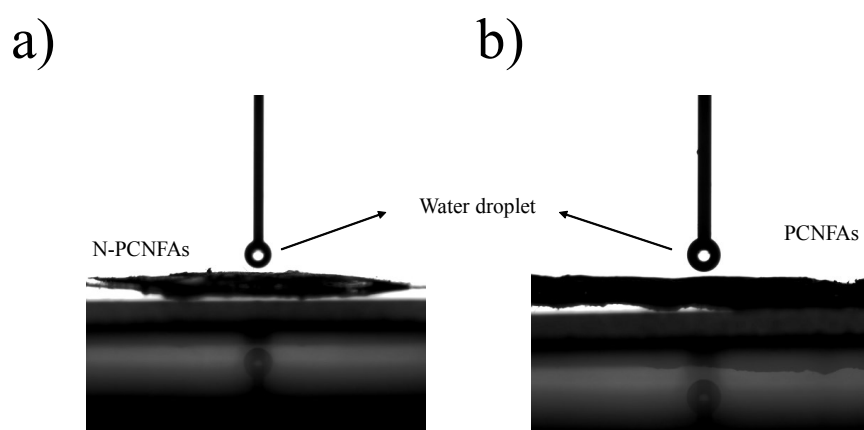


Fig. S9 GIF images of the interaction between the water droplet and (a) N-PCNFAs/
(b) PCNFAs (The GIF image would play by double-click on the image)

Through the GIF images, we could find that N-PCNFAs had a stronger interaction with the water droplet compared with PCNFAs, which was due to more N/O contained functional groups existing in N-PCNFAs as shown in Table S3. And it could help improve the wettability of N-PCNFAs in the aqueous electrolyte.

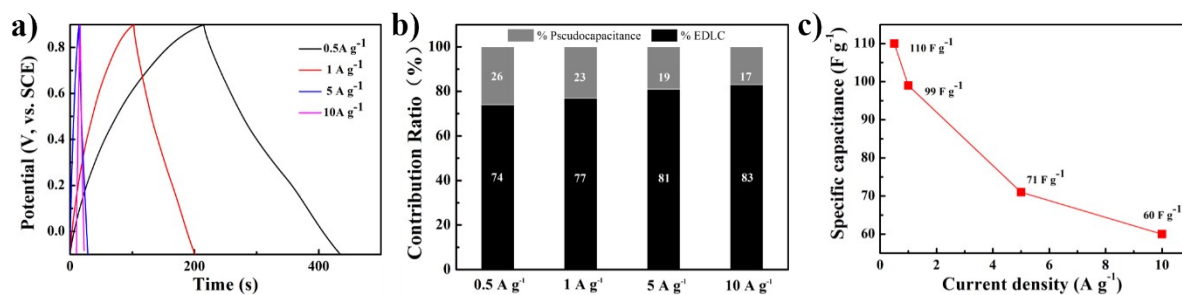


Fig. S10 Electrochemical performances of PCNFAs. (a) Galvanostatic charge-discharge curves, (b) the percentage of capacitance from EDLC and pseudocapacitance and (c) specific capacitance at different current densities.

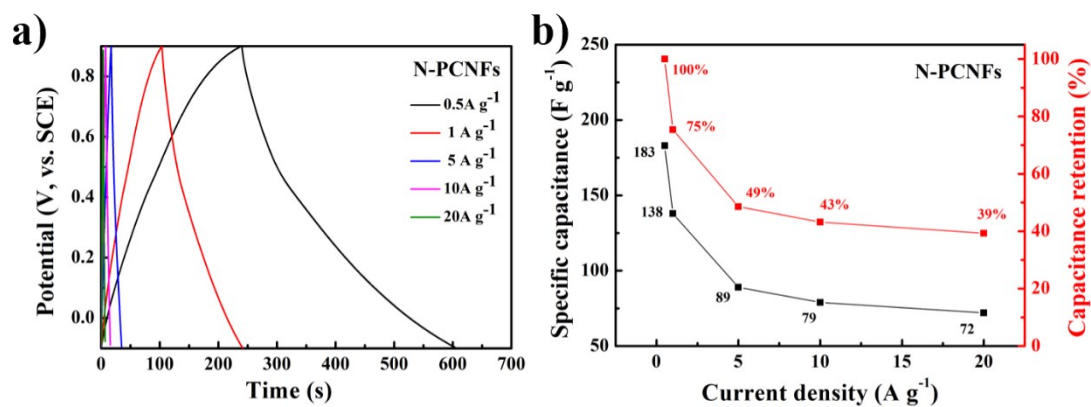


Fig. S11 Electrochemical performances of N-PCNFs. (a) Galvanostatic charge-discharge curves, (b) specific capacitance and corresponding rate capability at different current densities.

N-PCNFs was the sample of milled N-PCNFAs. To examine its electrochemical properties, N-PCNFAs was milled with acetylene black and polytetrafluoroethylene (PTFE) at a weight ratio of 80:10:10 in ethanol, and then the as-obtained slurry was coated onto 304 stainless steel mesh which was pressed at 10 MPa to get the working electrode. Then, the working electrode was tested using a three-electrode system with 1 M H₂SO₄ as the electrolyte.

Table S1 Pore parameters of N-PCNFAs and PCNFAs

Samples	Specific surface area (BET, m ² g ⁻¹)	Average pore diameter (DFT, nm)	Pore volume (DFT, cm ³ g ⁻¹)
N-PCNFAs	401.8	0.97	0.257
PCNFAs	265.3	0.97	0.169

Table S2 Atomic percentage (at%) of C, O and N in N-PCNFAs and PCNFAs

	C (at%)	N(at%)	O(at%)
N-PCNFAs	83.81	2.68	13.51
PCNFAs	92.58	1	6.42

Table S3 The ratio of N-5, N-6, N-Q and oxide N in the N1s signal

	N-6 (%)	N-5(%)	N-Q(%)	Oxide N(%)
N-PCNFAs	58.4	8.6	19.5	13.5
PCNFAs	9.9	30.4	59.6	0

Table S4. The ratio of sp², sp³, C-N/C-O, C=O and N-C=O/COOR in the C1s signal

	sp ² (%)	sp ³ (%)	C-N/C-O (%)	C=O (%)	N-C=O/COOR (%)
N-PCNFAs	58.0	5.5	11.6	10.4	14.5
PCNFAs	63.4	5.9	8	8.9	13.8